Atmospheric Pollution Research 4 (2013) 199-207
Technical Note

Atmospheric Pollution Research
www.atmospolres.com

Non–linear analysis of short term variations in ambient visibility

Ankit Tandon [1,2], Shweta Yadav [1], Arun K. Attri [1]

[1] *School of Environmental Sciences, Jawaharlal Nehru University, New Delhi – 110067, India*
[2] *School of Earth & Environmental Sciences, Central University of Himachal Pradesh, Dharamshala, Dist. Kangra, Himachal Pradesh – 176215, India*

ABSTRACT

Ambient visibility is a complex manifestation arising out of interactions among many atmospheric variables, including ambient aerosol load, and region specific geophysical characteristics. To functionally relate visibility impairment in Delhi region during winter months–months marred with poor visibility conditions–a novel experiment was designed to relate visibility with ambient aerosol load ($PM_{2.5}$), and relevant meteorological variables: dew point temperature (D_p), height of planetary boundary layer (PBL), ambient temperature (T), relative humidity (RH), wind speed (WS) and wind direction (WD). Time series data sets of Visibility(*t*) and other variables were subjected to non–linear decomposition using Empirical Mode Decomposition Method (EMD), enabling to obtain total cyclic and acyclic–trend components embedded in all data–sets. Extracted total cyclic visibility components were functionally related with the corresponding components associated with $PM_{2.5}$ load and meteorological variables. Decomposed acyclic–trend component of the visibility, representing time dependent acyclic trend (AT), was separately related with the corresponding AT components of the considered meteorological variables. The decomposed components of the visibility (total cyclic and AT) were subjected to multiple linear regression to establish a functional relationship between them and a set of variables among the considered variables. The analysis suggests that acyclic–trend associated with Visibility(*t*) can be predicted better as opposed to the Visibility$(t)_{cyclic}$ component.

Keywords: *Visibility, non–linear analysis, empirical mode decomposition, meteorological variables, $PM_{2.5}$*

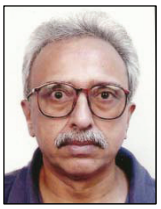

Corresponding Author:
Arun K. Attri
☎ : *+91-9560-461930*
✉ : *attri@mail.jnu.ac.in*
attriak@gmail.com

Article History:
Received: 07 December 2012
Revised: 10 March 2013
Accepted: 11 March 2013

doi: 10.5094/APR.2013.020

1. Introduction

Impairment of visibility, during winter, is a common feature in the region encompassing Indo–Gangetic planes. Both number of days and the hours during the day for which low visibility conditions persist have gone up in the last two decades (De et al., 2005). These conditions cause severe disruption in the air, rail and road traffic, and result in the loss of human lives, besides inflicting considerable economic loss (Badarinath et al., 2009).

Given the pervasive impact of visibility on the routine and essential human activities, it has been a focus of scientific investigation for considerable time in relation to the role of local and regional meteorological variables (Petterssen, 1956; Doran et al., 1999; Knapp, 1999; Smirnova et al., 2000; Smith and Benjamin 2002; Benjamin et al. 2004; Gultepe and Issac, 2006; Badarinath et al., 2009; Gultepe et al., 2009; Gultepe and Milbrandt, 2010; Chmielecki and Raftery, 2011; Tiwari et al., 2011). Deriving a universal functional relation between the visibility and meteorological variables is a challenging scientific problem; even a forecasting of the visibility over short duration is a tricky proposition (Chmielecki and Raftery, 2011).

Numbers of different functional forms of the visibility, explained with the help of meteorological variables, have been reported (Doran et al., 1999; Knapp, 1999; Smirnova et al., 2000; Smith and Benjamin 2002; Benjamin et al. 2004; Gultepe and Issac, 2006; Badarinath et al., 2009; Gultepe and Milbrandt, 2010; Tiwari et al., 2011). Broadly, different approaches were used to functionally relate the visibility with different combinations of atmospheric variables: (a) multiple linear regression, (b) numerical weather prediction involving remote sensing meteorology, and (c) simple statistical approach involving ambient aerosol load, dew point (DP), and relative humidity (RH). The phenomenon of acute visibility impairment is often transient, and occurs over short duration, lasting for few days or weeks. The visibility trend estimate is an important information of interest; a daunting task, as the time series data represents the amalgamation of the time dependent short term trends, the modulations and the noise; i.e. in addition to the presence of non–linearity. Modulations represent affects of many physical processes occurring over a wide time scale (seconds, hours, days, weeks). Mathematically the trends can be estimated, even in the presence of the natural modulations and the noise, but it requires a large number of time series observations, taken over many years (Weatherhead et al., 1998); a requirement unavailable in case of the short duration (few days to weeks) of acute visibility phenomenon. It is also important to keep in mind that the visibility impairment conditions in the environment occur at different locations for varying durations, irrespective of the fact that each location differs considerably in terms of the involved region specific geophysical and meteorological causal variables leading to the impaired visibility: e.g. ambient aerosol load; dew point (DP); planetary boundary layer (PBL); relative humidity (RH); ambient temperature (T); wind direction (WD); wind speed (WS); cloud water content etc. Given the limited number of observations obtained over the acute visibility impaired conditions and the complexity embedded in the data, it is imperative to use a suitable method which is able to visualize the time dependence of visibility as two distinct components: (i) cyclic modulations caused by the variability in the causal natural variables over different temporal scale (hours, diurnal, weeks); and (ii) the time dependent acyclic trend (AT)

intrinsically adapted to the data. This, in present paper, was achieved by using non–linear analytical approach which is adequate to decompose cyclic modulations from the embedded acyclic trends (ATs) present in the data set. The method is adequate to handle the presence of any non–linearity associated in the data sets and can be applied to time series data having observations >30 (Huang et al., 1998). In principle, such analysis would allow to relate the cyclic part of the visibility with the corresponding cyclic components embedded in the variables (aerosol load and meteorological variables) considered to seek a relation. Similarly, AT component of the visibility can be functionally related with the corresponding AT component present in the explaining variables.

The designing of experiment to understand the impaired wintertime visibility in the region of this study, and the used method of analysis of the data allowed us to relate the embedded cyclic and acyclic components with those present in the corresponding meteorological variables and aerosol load. Set of meteorological variables considered to functionally explain cyclic and acyclic components of the visibility were decided on the basis of the calculated Kendall's correlation, prior to the establishing of a multiple linear regression functional relation.

The stated objectives of decomposing (a) cyclic and (b) acyclic trend (AT) components present in the visibility and the considered meteorological variables was achieved by subjecting respective data–sets to Empirical Mode Decomposition (EMD); the method is not constrained by the presence of non–linearity and non–stationarity present in the data–sets (Huang et al., 1998; Wu et al., 2011). Decomposed cyclic and acyclic trend components of the visibility data set were analyzed with respect to the corresponding counterparts present in the meteorological variables considered as independent variables. The results from this analysis clearly establish that visibility has two components (cyclic and acyclic trend) and each is influenced by the corresponding (cyclic and acyclic) components present in the considered independent variables.

2. Experimental Design, Data Collection, and Methodology

Functional relationship of visibility with $PM_{2.5}$ load and meteorological variables being the main focus, the designed experiment was conducted in Delhi to collect $PM_{2.5}$ aerosol load; where, during winter (December and January) this region is inflicted with severe visibility impaired conditions. These conditions extend to the most of the north–western part of India, and persist over many days to a few weeks. The site selected was representative of the impaired visibility conditions during winter. High aerosol load in the ambient environment of Delhi region is a year round phenomenon, and collection of every six hourly $PM_{2.5}$ load was an important aspect to capture cyclic variations (diurnal) present in the load as opposed to the conventionally 24 hourly load collections (Tandon et al., 2008; Tandon et al., 2010). Sample collection time <6 hours sample^{-1} would be a better alternative, but the aerosol mass collection decreases significantly with decrease in the collection time. For accurate mass measurement of the load 6 hour collection time was found to be optimum. As ambient aerosol load is an important factor in relation to the ambient visibility (Seinfeld and Pandis, 2006), it was not only important to collect 6 hourly sample collection of the $PM_{2.5}$ load, but it was also crucial to collect the samples in a discrete time series.

2.1. Description of sampling site

The capital region of Delhi is geographically located between 28°25'N and 28°53'N; 76°50'E and 77°22'E at 216 m above MSL in the northern part of India. It has a semi–arid climate, influenced by the Himalayan ranges to the north, Thar Desert to the west, the central hot plains to the south and cooler hilly region to the northeast. Delhi has the dubious distinction of being one of the most polluted cities in the world and is afflicted with unusually high concentrations of aerosols in the lower atmosphere (Yadav and Rajamani, 2006; Tandon et al., 2008; Tandon et al., 2010). Large amounts of wind–blown dust envelops the city during hot and long summer and the onset of winter season brings a regular feature of ground–based temperature inversion, which further amplifies the load on account of the calm wind regime and low planetary boundary layer (PBL) conditions (Yadav et al., 2013). The location selected for this experiment, Jawaharlal Nehru University (JNU) is a 1 000 acre lush green campus having large patches of scrub and forest land, and comparatively less traffic load inside the campus. JNU is a known receptor site (Singh et al., 1997) in the south Delhi ridge area, which forms a plateau of 250–300 m elevation above the mean sea level and is approximately 100 m above the surrounding area. Sequential six hourly samples, over twenty days, of $PM_{2.5}$ were collected on the rooftop of a building at 15 m height. The numbers of samples collected over twenty days were considered sufficient for EMD based determination of the embedded cyclic components and acyclic trends present in the $PM_{2.5}$ load time series.

2.2. Sample collection

$PM_{2.5}$ aerosol samples were collected, using Mass Flow Controlled Fine Particulate sampler (Envirotech – APM 550 MFC), equipped with Well Impactor Ninety Six (WINS). The samples were collected on Whatman PTFE filters (46.2 mm) at a constant flow rate of 16.7 L min^{-1}. The sample collection was done from 15th December, 2010 to 3rd January, 2011. Four samples/day were collected over 6 hour duration (00:00–06:00, 06:00–12:00, 12:00–18:00, 18:00–00:00 hours). Concentration of the $PM_{2.5}$ samples was estimated by gravimetric determination of the collected aerosol mass, using electronic microbalance with 0.01 mg accuracy.

2.3. Meteorological variables

Half hourly values of meteorological variables; visibility (V), temperature (T), dew point (DP), relative humidity (RH), wind direction (WD) and wind speed (WS), were obtained from Wyoming University (WU, 2012)http://weather.uwyo.edu/surface/meteogram/), and 3–hourly values for Planetary Boundary Layer (PBL) were taken from Air Resources Laboratory, National Oceanic and Atmospheric Administration (NOAA, 2012) (http://www.arl.noaa.gov/ READYamet.php) for the region of this study; the data obtained is from an observatory located close to the aerosol collection sampling site. The half hourly and 3–hourly values were averaged over 6 hours into a discrete time series sequence to match with the time points of the collection of the aerosol load.

2.4. Analysis of visibility and meteorological data: determination of total cyclic component

The visibility and meteorological data was decomposed into (a) cyclic and (b) acyclic trend components by using EMD, the details of the methodology and the steps involved are provided in the seminal work done by Huang et al. (1998). Presence of the time dependent modulations, and trend embedded in the respective data–sets, at gross level, can be perceived from the corresponding plots shown in Figure 1; and they can be represented by following general expression as a function of time (t):

$$\text{Data}(t) = \text{Total Cyclic}(t) + \text{Acyclic Trend}(t) \quad (1)$$

The modulations associated with the respective data–set (Figure 1) can be expressed as the sum of all Internal Mode Functions (IMFs) present in the respective data–set. The extracted IMF, in a given data, would represent a modulation having distinct average period in hours (hr) and average amplitude (hr^{-1}). The sum of the extracted IMFs present in a data would represent total cyclic components over the time domain of the data set, and it can be represented by following relation:

$$\text{Total Cyclic}(t) = \sum_{j=1}^{M} \text{IMF}(t)_j \quad (2)$$

In above relation, *M* represents the number of IMFs associated in a respective data–set, each extracted by using EMD. The determined oscillatory modes from the data conforms to following two conditions: (i) given IMF, over the range of data time domain, manifests equal number of extrema and zero crossings, or they differ by one; (ii) over the data range the mean value of the envelops defined by local maxima and minima is close to zero. Statistically, the extracted mode conforming to the definition of IMF can be ascertained (Wu et al., 2011). Extraction of different modes (IMFs) is initiated by determining the minima and maxima points present in the data–set having oscillations; all points representing maximas are fitted by using cubic spline function and the same exercise is repeated to get the spline fit through all minima points. The fitted spline functions to the points representing maxima and minima are designated as upper $up_e(t)$ and lower envelop $lw_e(t)$, respectively. The average of these two, $m_1(t) = [(up_e(t) + lw_e(t))/2]$, is subtracted from the original data–set(t) to provide the first approximate representation of $\text{IMF}_1(t)$ designated as $h_1(t)$.

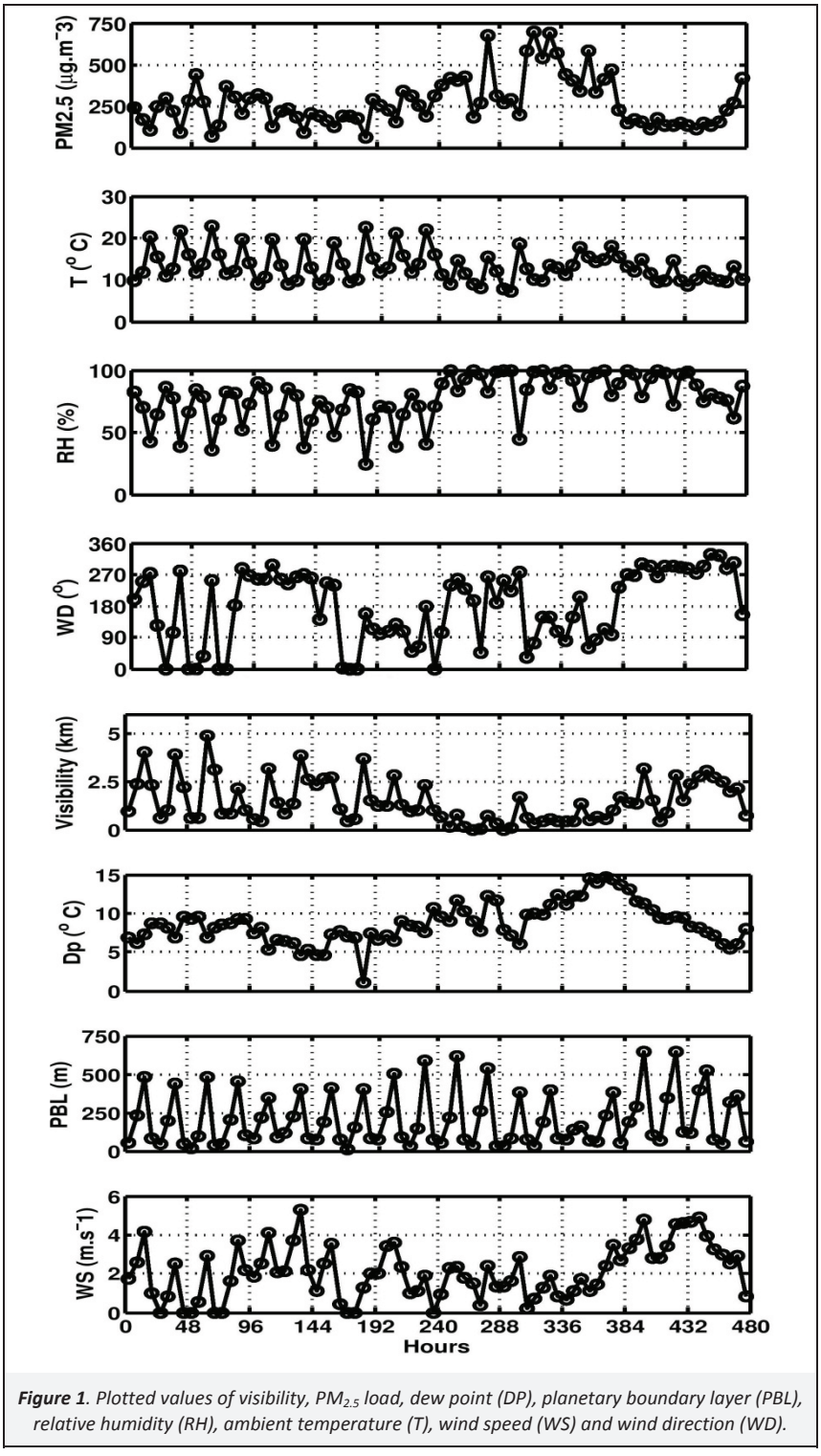

***Figure 1**. Plotted values of visibility, $PM_{2.5}$ load, dew point (DP), planetary boundary layer (PBL), relative humidity (RH), ambient temperature (T), wind speed (WS) and wind direction (WD).*

$$\text{Data Set}(t) - m_1(t) = h_1(t) \quad (3)$$

Further processing of $h_1(t)$, by using repeated sifting, is done by treating it in same manner as was done in the case of the initial data–set till an acceptable decomposed highest frequency IMF_1 is obtained. Required number of siftings for processed IMF_1 is decided by following a pre–set condition for standard deviation (SD) between $h_{1(k-1)}(t)$ and $h_{1k}(t)$, where k represents the sifting number; SD is expressed as:

$$SD = \sum_{t=0}^{T} \left[\frac{\left| h_{1(k-1)}(t) - h_{1k}(t) \right|^2}{h_{1(k-1)}(t)^2} \right] \quad (4)$$

In the present analysis SD<0.1 was used as a stoppage criteria for the sifting and to accept h_{ik} as the IMF_1 (Huang et al., 1998). $IMF_1(t)$, represents highest frequency oscillations present in the data–set(t); lower frequency IMF_S (IMF_2, IMF_3...IMF_M), in decreasing order of frequency are processed from the residuals obtained at each stage: i.e. subsequent to the subtraction of processed IMF_j from the preceding data–set (or residuals). The procedure is repeated until no further IMFs could be extracted from the residuals, or the residuals manifest a monotonic character or have at maximum one extremum. The sum of residuals $r_n(t)$ and decomposed $\Sigma(IMF_j)$ could be statistically compared with the original data set of Visibility(t) to assess the accuracy of the EMD method, and ascertain the extent of data explained by this analysis. The data–set (t), subsequent to the decomposition of all the IMFs can be expressed as:

$$\text{Data set}(t) = \sum_{j=1}^{M} \text{IMF}(t)_j + \text{residuals}(t)_n \quad (5)$$

2.5. Acyclic–trend estimation

The residuals$(t)_n$, in Equation (5) represents the mode of data where well defined periodic variations are absent, as they are already accounted by total cyclic components (ΣIMF_j). Residuals, over the data time domain, represent adaptive or acyclic–trend (Huang et al., 1998; Wu et al., 2007). In present context, in the analysis of the visibility and the respective causal meteorological variables, the total cyclic components present in the respective data set will correspond to ΣIMF_j. AT component can be extracted subsequent to the subtraction of ΣIMF_j from the original data–set; i.e. residuals from which further extraction of IMF is not possible.

2.6. Minimizing end effects, over–shoot and under–shoot

Cubic spline fit to the oscillating time series data–sets, during repeated sifting, suffers from the problem of end effects and over–shoot, which in turn infects inward values. To minimize the problem of over–shoot and under–shoot we used piecewise cubic Hermite interpolating polynomial (Fritsch and Carlson, 1980; Kahaner et al., 1988) to fit the $lw_e(t)$ and $up_e(t)$ peak values; this was effective in eliminating the stated problem as compared to the use of simple cubic spline fit. End effect problem was eliminated by taking two steps: (1) data at the start of the series under analysis was padded by adding data points from the same set by adjusting the first and the last value in respective data–set with respect to the calculated slope of first two and the last two points. This consideration was found to be effective in minimizing the end effect, and it controlled the infection of inner values during repeated sifting procedure due to the progression of end effects inward. These calculations were done on visibility, $PM_{2.5}$, DP, PBL, RH, T, WD and WS data sets to extract embedded total cyclic component (ΣIMF_j) and acyclic trend component in respective data–set. All calculations were done using MATLAB 7.1 platform.

3. Results and Discussion

EMD analysis of the Visibility(t) and meteorological variables ($PM_{2.5}$, DP, PBL, RH, T, WD, WS) data–sets revealed five IMFs (see the Supporting Material, SM, Figure S1, showing representative IMFs, and acyclic–trend extracted from the visibility data–set). Each IMF, in respective data–sets, has distinct average period and average amplitude. For further analysis, sum of all the IMF_S, (ΣIMFs), that represent the total cyclic component associated with the respective data sets, were used.

3.1. Criteria for selecting the meteorological variables to explain visibility using multiple linear regression

Total cyclic component associated with the visibility was grouped with the total cyclic components determined in the meteorological variables (Section 2.4); and similarly a separate data–set of the acyclic–trends in the visibility was grouped with the corresponding acyclic–trends present in the meteorological variables (Section 2.5). As a first step, to ensure the relevance of considered meteorological variables to explain the visibility, Kendall's correlation coefficient between variables (see the SM, Table S1 for total cyclic and Table S2 for ATs) was determined. This step was considered necessary to select the appropriate combination of independent variables from all the considered variables ($PM_{2.5}$, DP, RH, T, WS and WD) on the basis of the calculated statistical co–linearity between the variables to establish a functional relation with the Visibility(t) (cyclic or acyclic part). However, it is important to state that the absence of the correlation between Total cyclic components may arise due to the presence of a lag between the variables with respect to their respective periodicity in their total cyclic profile.

For ATs component, on the basis of Kendall's correlation between different variables, it was possible to form different groups of strongly correlating variables (Kendall's correlation >0.9 and having statistical significance at 0.01 level): (1) $PM_{2.5}$ and DP (0.965); (2) PBL and RH (0.934); (3) WD and WS (0.929); and (4) temperature did not show strong correlation with any other variable considered. It is evident that strong correlation between different groups of the independent variables will affect the multiple linear regression function on account of the statistical co–linearity, while fitting the visibility's AT component.

3.2. Functional relation of the cyclic component of visibility with meteorological variables

Multiple regressions fit to total cyclic visibility component, with the total cyclic component present in the independent variables was done by excluding those variables showing strong statistical co–linearity. The variables considered were: $PM_{2.5}$, DP, T and WS. Equation for Multiple Linear Regression fit explaining the total cyclic component of the visibility can be expressed as:

$$\begin{aligned} \text{Total Cyclic}(t)_{\text{visibility}} &= -0.002 \times \text{PM}(t)_{2.5\,Cyclic} - 0.159 \times \text{DP}(t)_{\text{Cyclic}} \\ &\quad + 0.167 \times \text{T}(t)_{\text{Cyclic}} + 0.128 \times \text{WS}(t)_{\text{Cyclic}} \end{aligned} \quad (6)$$

The estimated error in the determined coefficients, respectively, was ±0.001, ±0.028, ±0.017, and ±0.050; adjusted R^2 for the fit was 0.794. Figure 2 shows the plot of total cyclic visibility component obtained from the EMD analysis of the visibility data, and the same fitted to the multiple regression fit by Equation (6). The plot also show the spread in the fitted values obtained by considering the statistical uncertainty in the fitted coefficients, to the independent variables. The Equation (6), explains changes in the total cyclic component of the visibility involving the corresponding cyclic variations present in the explaining independent variables. Estimated coefficient of $PM_{2.5}$, having negative sign, suggests that any increase in the aerosol load will result in the

decrease in the cyclic component of the visibility; the same is implicit from the dew point temperature, which also has fitted a negative coefficient value. On other hand, an increase in T and WS suggests the increase of visibility's cyclic components. The role of the explaining variables considered to explain the cyclic visibility component is evident from the fitted functional relation, however the extent to which the decrease or increase in the cyclic part of the visibility is affected by the respective variable can only be done after normalizing the independent variables within the range they vary over the time domain of the data–set as they have different units; however, the overall effect of these variables in explaining visibility will not alter. The statistics of the regression fit to explain the cyclic component of the visibility by the corresponding part present in the explaining variables ($PM_{2.5}$, DP, T and WS) is acceptable (R^2=0.794), which suggests that unexplained cyclicity associated with the visibility may be on account of the presence of the noise component. The upper and lower bound error (95% confidence) in functionally explaining the cyclic part of the visibility is shown by the shaded part surrounding the fitted function to the EMD decomposed total cyclic visibility values.

3.3. Functional relation of the acyclic trend component of the visibility with the meteorological variables

Profiles of AT components extracted from the visibility data using EMD, and all independent variables considered are shown in Figure 3, it is noted that all profiles manifest acyclic trend (not linear trend) present in the respective variable. This suggests that the conventional analysis based on the estimation of linear trends in the climatic variable is presumptuous. The ATs extracted from visibility, aerosols ($PM_{2.5}$), DP, PBL, RH, T, WD and WS, on the other hand provides timeline of the changes associated with the variables; any addition of new data would not alter the determined AT, unlike the conventional linear trend estimates (Huang et al., 1998). For instance, eye balling of the AT profiles provide immediate appreciation for impaired visibility (around 300 hours, Figure 3, Panel 1) and its strong correlation with AT present in aerosols, DP and RH profiles.

Keeping in view the strong correlation between different groups of the explaining independent variables used to elucidate AT in the visibility (Section 3.1), the statistical co–linearity based criteria was used to exclude variable overlap. Multiple regression function fit to the AT component of the visibility can be expressed as:

$$\begin{aligned}\text{Visibility}(t)_{\text{Acyclic}-\text{Trend}} = &-0.549\times \text{DP}(t)_{\text{Acyclic}-\text{Trend}} \\ &+0.017\times \text{PBL}(t)_{\text{Acyclic}-\text{Trend}} \\ &+0.887\times \text{WS}(t)_{\text{Acyclic}-\text{Trend}}\end{aligned} \quad (7)$$

Standard error in the fitted coefficients in Equation (7) was ≤0.001, adjusted R^2 approached to 1.0, and the standard error of estimate in the fitted model value equaled 0.00272. It is evident that the results of the regression fit explained fully the AT component associated with the visibility. The coefficients manifested insignificant error (0.001). The fitted coefficient of DP, having negative sign, suggests the decrease in the visibility trend with an increase in DP. Acyclic trend in the visibility would improve with an increase in the PBL height and an increase in the WS. The absence of $PM_{2.5}$ from the fitted function was curious, it seems that the modulations in the aerosol load has more to do with the cyclic part of the visibility; the AT component of the visibility is plotted with the multiple regression based fit derived from Equation (7) in Figure 4. The fit is enveloped by the uncertainty spread region at 95% confidence; extracted acyclic trend in the visibility can be estimated with high accuracy. It is interesting to note that DP and WS affect both components of visibility. Visibility's functional form, which includes both components, can be expressed as Equation (8):

$$\text{Visibilty}(t) = \text{Visibilty}(t)_{\text{Cyclic}} + \text{Visibility}(t)_{\text{Acyclic}-\text{trend}} \quad (8)$$

where, the first part on the right–hand side of the equation is a function of $PM_{2.5}$, DP, T, WS; and the second part of DP, PBL and WS. Equation (8) explains reasonably well the role of meteorological variables affecting ambient visibility and it is implicit that DP, WS are independent variables, and they have maximum effect in lowering the visibility. The complete functional forms of the two sub functions in the Equation (8) are given by the Equations (6) and (7). The Visibility data fitted to Equation (8) is shown in Figure 5. Upper and lower confidence band at 95% level is shown by taking into account the uncertainty in the fitted coefficients of Visibility$(t)_{\text{cyclic}}$ and Visibility$(t)_{\text{Acyclic–trend}}$ functions.

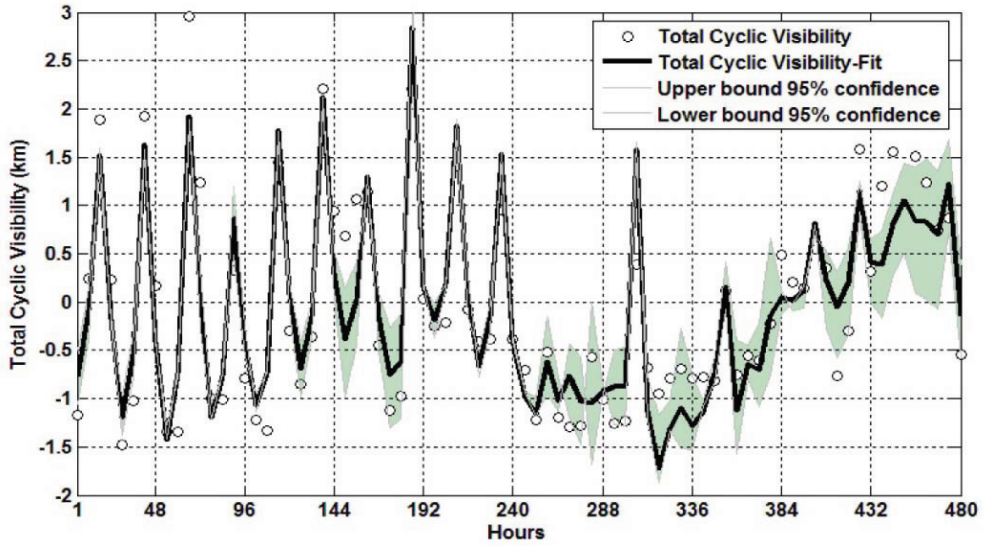

***Figure 2**. Total cyclic visibility values obtained after subtracting the acyclic-trends from the original visibility data (circles) is fitted to multiple linear regression (sold line) function ($PM_{2.5}$, DP, T, WS). The shaded envelop surrounding the regression fit represent the uncertainty (95% confidence) in predicting the Visibility$(t)_{cyclic}$.*

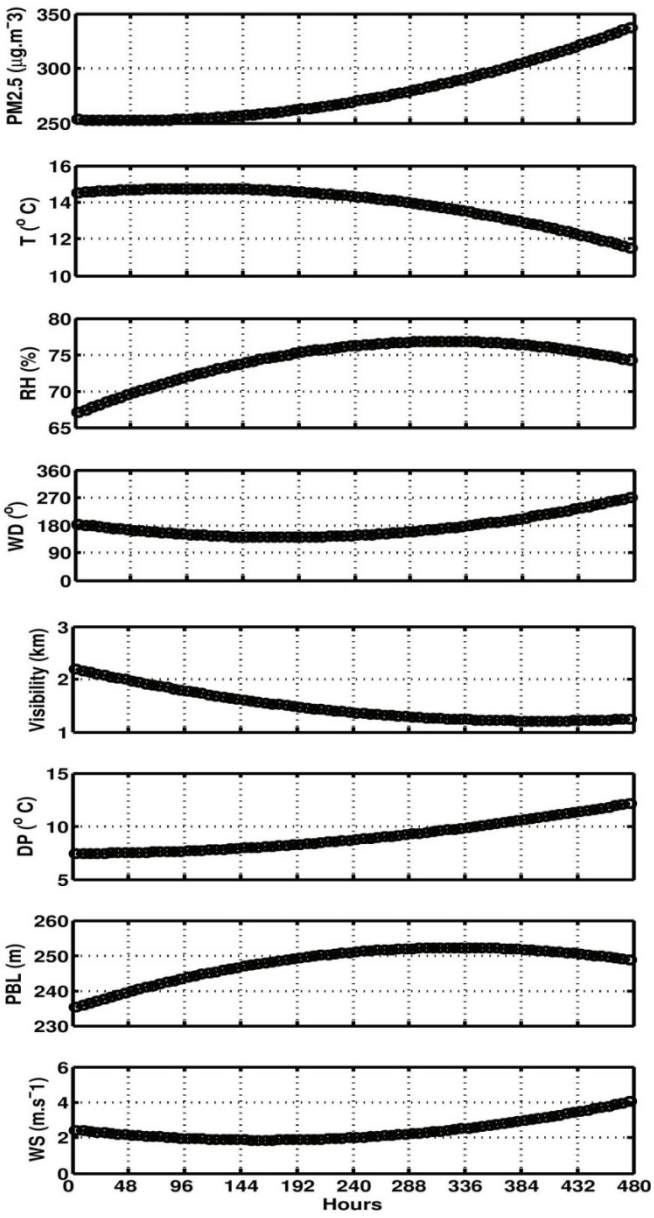

***Figure 3**. Extracted acyclic trends present in the visibility data and independent variables considered ($PM_{2.5}$ load, DP, T, PBL, RH, WS and WD) to explain Visibility(t).*

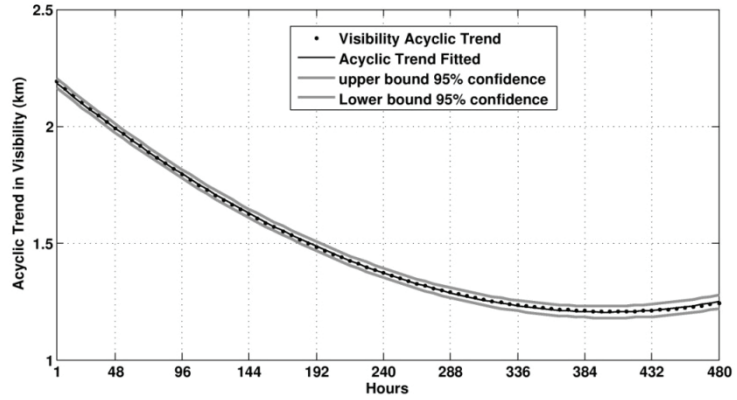

***Figure 4**. Acyclic trend component values (black dots) fitted (black line) to multiple linear regression function (DP, PBL and WS); R^2 of the fit approaches 1.0. The fit is surrounded with the region (thick grey lines) showing uncertainty (95% confidence) in predicting $Visibility(t)_{Acyclic\text{-}trend}$.*

4. Conclusion

The strategy adopted to consider the modulations and the embedded trend encountered in the visibility observations as two distinct attributes reveal that; (1) the total cyclic component are influenced by the separate set of environment variables ($PM_{2.5}$, DP, T and WS), and (2) the acyclic trend involves the role of DP, PBL and WS. Multiple regression fit based function to predict Visibility$(t)_{cyclic}$ does not explain fully all the associated cyclic component, which is evident from the uncertainty band drawn around the fitted function. Unexplained cyclic part of the data in the form of residuals plotted in Figure 6 (upper panel) suggests that the residuals are randomly distributed and does not display any systematic trend. The plotted autocorrelation function (ACF) for the residuals (Figure 6, lower panel) substantiate the preceding inference; the residuals attributes can be assigned as noise, which would also limit the predictability of the Visibility$(t)_{cyclic}$.

The function obtained to explain Visibility$(t)_{Acyclic–trends}$, on other hand explains well the predictability of the embedded trends in the visibility data. The residuals, the unexplained part of acyclic–trend data, were small (Figure 7, upper panel). However, there is clear evidence of systematic variation associated with the residuals in this case and same cannot be categorized as noise. The plotted ACF with lag of residuals does not decays gradually in this case (Figure 7, lower panel), which is indicative of the presence of persistence in the Visibility$(t)_{Acyclic–trend}$. It can be inferred that the presence of persistence would allow the better predictability of acyclic–trends from the attributes of involved causal variables (DP, PBL and WS). Suggested approach to understand the manifestation of atmospheric processes, as in case of the visibility, is not limited to the presumptuous fit done to the a priori model form; and is not limited on account of the presence of the non–linearity in the data.

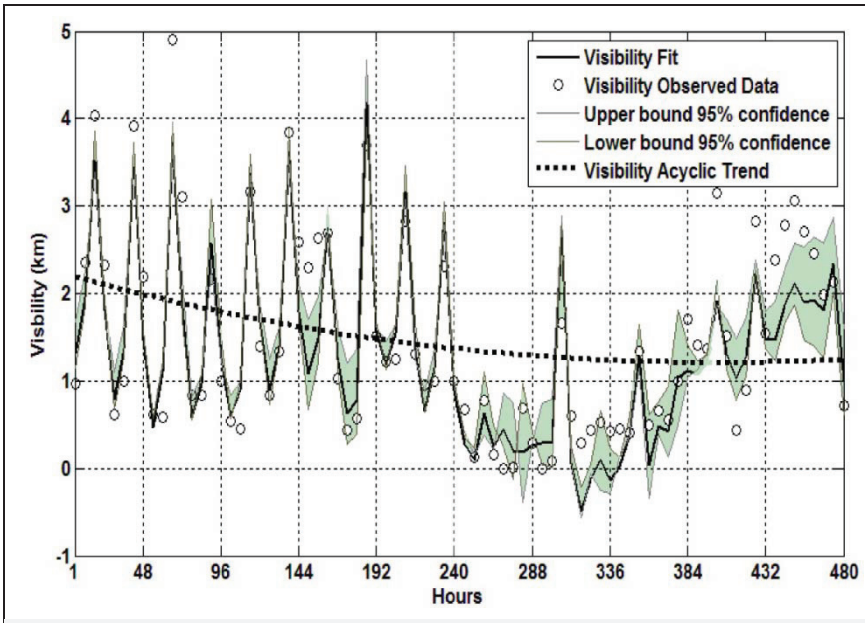

Figure 5. *Plot showing the fitted (black line) function to the Visibility(t) data points (circles), and acyclic trend fit (dotted line). The fit includes total cyclic + acyclic components of the Visibility(t). The uncertainty involved is shown by the shaded region (95% confidence) surrounding the fit.*

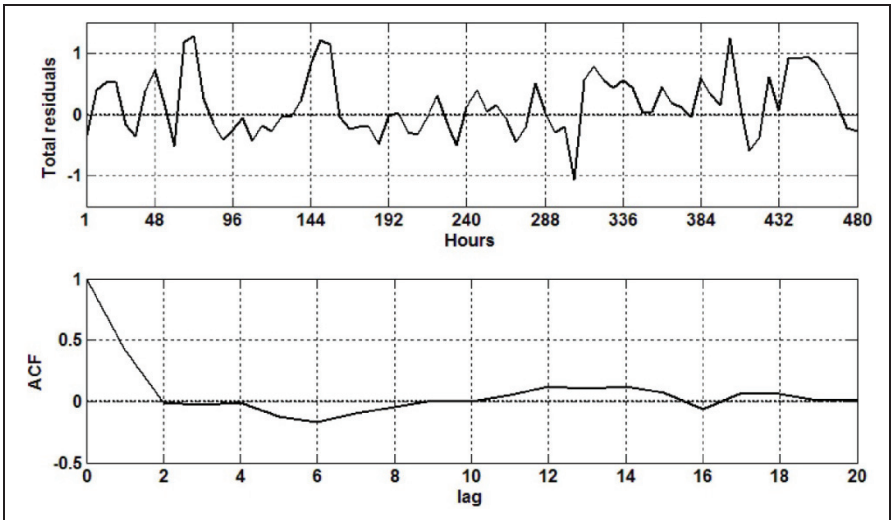

Figure 6. *Residuals obtained from the difference between the regression fit to Visibility(t) data (thick black line) and the original observed visibility data are shown in upper panel. The lower panel of the figure shows the plotted ACF with lag.*

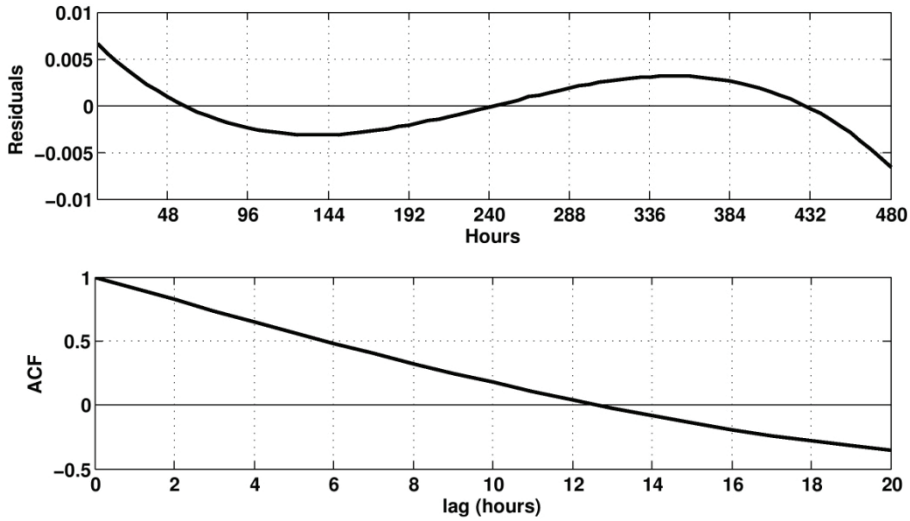

Figure 7. *Residuals obtained from the difference between the Visibility(t)$_{Acyclic\text{-}trend}$ data and the fitted function to these values are plotted in the upper panel. Lower panel shows the plot of ACF with lag.*

Acknowledgement

Authors extend their gratitude to National Oceanic and Atmospheric Administration and Wyoming University for providing data on meteorological variables used in this work. AT is thankful to Department of Science and Technology, Government of India for the financial assistance provided to him as young scientist, in the form of a research project. SY acknowledges financial assistance provided by the University Grant Commission in the form of Senior Research Fellowship. AKA appreciates the financial support provided in the form of a project by Council for Scientific and Industrial Research, India. We appreciate the critical review of this manuscript done by three anonymous referees, which has contributed in the significant improvement of this manuscript.

Supporting Material Available

Estimated Kendall's correlation between meteorological variables and $PM_{2.5}$ load for total cyclic components (ΣIMF_s) (Table S1), Estimated Kendall's correlation between meteorological variables and $PM_{2.5}$ load Acyclic–trend components (Table S2), Representative plot of EMD based extraction of five IMFs (Figure S1). This information is available free of charge via Internet at http://www.atmospolres.com.

References

Badarinath, K.V.S., Kharol, S.K., Sharma, A.R., Roy, P.S., 2009. Fog over Indo—Gangetic plains — a study using multisatellite data and ground observations. *IEEE Journal of Selected Topics in Applied Earth Observations and Remote Sensing* 2, 185—195.

Benjamin, S.G., Devenyi, D., Weygandt, S.S., Brundage, K.J., Brown, J.M., Grell, G.A., Kim, D., Schwartz, B.E., Smirnova, T.G., Smith, T.L., Manikin, G.S., 2004. An hourly assimilation — forecast cycle: the RUC. *Monthly Weather Review* 132, 495—518.

Chmielecki, R.M., Raftery, A.E., 2011. Probabilistic visibility forecasting using Bayesian Model averaging. *Monthly Weather Review* 139, 1626—1636.

De, U.S., Dube, R.K., Prakasa Rao, G.S., 2005. Extreme weather events over India in the last 100 years. *The Journal of Indian Geophysical Union* 9, 173—187.

Doran, J.A., Roohr, P.J., Beberwyk, D.J., Brooks, G.R., Gayno, G.A., Williams, R.T., Lewis, J.M., Lefevre, R.J., 1999. The MM5 at the AF Weather Agency — new products to support military operations. *Proceedings of 8th Conference on Aviation, Range, and Aerospace Meteorology*, American Meteorological Society, January 10, 1999, Dallas, TX, pp. 115—119.

Fritsch, F.N., Carlson, R.E., 1980. Monotone piecewise cubic interpolation. *SIAM Journal on Numerical Analysis* 17, 238—246.

Gultepe, I., Milbrandt, J.A., 2010. Probabilistic parameterizations of visibility using observations of rain precipitation rate, relative humidity, and visibility. *Journal of Applied Meteorology and Climatology* 49, 36—46.

Gultepe, I., Issac, G.A., 2006. Visibility versus precipitation rate and relative humidity. *Proceedings of 12th Cloud Physics Conference*, American Meteorological Society, Madison, WI.

Gultepe, I., Pearson, G., Milbrandt, J.A., Hansen, B., Platnick, S., Taylor, P., Gordon, M., Oakley, J.P., Cober, S.G., 2009. The fog remote sensing and modeling field project. *Bulletin of the American Meteorological Society* 90, 341—359.

Huang, N.E., Shen, Z., Long, S.R., Wu, M.C., Snin, H.H., Zheng, Q., Yen, N.C., Tung, C.C., Liu, H.H., 1998. The empirical mode decomposition and the Hubert spectrum for nonlinear and non—stationary time series analysis. *Proceedings of the Royal Society A: Mathematical, Physical and Engineering Sciences* 454, 903—995.

Kahaner, D., Moler, C., Nash S., 1989. Numerical Methods and Software, Prentice Hall.

Knapp, D., 1999. An advanced algorithm to diagnose atmospheric turbulence using numerical model output. *Proceedings of the 16th Conference on Weather Analysis and Forecasting*, American Meteorological Society, Phoenix, AZ, January 16, 1999, pp. 79—81.

NOAA, 2012. Air Resources Laboratory. http://www.arl.noaa.gov/READYamet.php, accessed in December 2012.

Petterssen, S., 1956. *Weather Analysis and Forecasting*, McGraw—Hill, Book Inc., pp. 196-214.

Seinfeld, J.H., Pandis, S.N., 2006. *Atmospheric Chemistry and Physics: From Air Pollution to Climate Change*, John Wiley & Sons, New York, pp. 1126-1150.

Singh, A., Sarin, S.M., Shanmugam, P., Sharma, N., Attri, A.K., Jain, V.K., 1997. Ozone distribution in the urban environment of Delhi during winter months. *Atmospheric Environment* 31, 3421—3427.

Smirnova, T.G., Benjiman, S.G., Brown, J.M., 2000. Case study verification of RUC/MAPS fog and visibility forecasts. *Proceedings of the 9th Conference on Aviation, Range, and Aerospace Meteorology*, American Meteorological Society, September 11, 2000, Orlando, FL.

Smith, T.L., Benjamin, S.G., 2002. Visibility forecasts from the RUC20. *Proceedings of the 10th Conference on Aviation, Range, and Aerospace Meteorology*, American Meteorological Society, May 13, 2002, Portland, OR.

Tandon, A., Yadav, S., Attri, A.K., 2010. Coupling between meteorological factors and ambient aerosol load. *Atmospheric Environment* 44, 1237—1243.

Tandon, A., Yadav, S., Attri, A.K., 2008. City—wide sweeping a source for respirable particulate matter in the atmosphere. *Atmospheric Environment* 42, 1064—1069.

Tiwari, S., Payra, S., Mohan, M., Verma, S., Bisht, D.S., 2011. Visibility degradation during foggy period due to anthropogenic urban aerosol at Delhi, India. *Atmospheric Pollution Research* 2, 116—120.

Wu, Z.H., Huang, N.E., Wallace, J.M., Smoliak, B.V., Chen, X.Y., 2011. On the time—varying trend in global—mean surface temperature. *Climate Dynamics* 37, 759—773.

Yadav, S., Rajamani, V., 2006. Air quality and trace metal chemistry of different size fractions of aerosols in N–NW India — implications for source diversity. *Atmospheric Environment* 40, 698—712.

Yadav, S., Tandon, A., Attri, A.K., 2013. Monthly and seasonal variations in aerosol associated n—alkane profiles in relation to meteorological parameters in New Delhi, India. *Aerosol and Air Quality Research* 13, 287—300.

Weatherhead, E.C., Reinsel, G.C., Tiao, G.C., Meng, X.L., Choi, D.S., Cheang, W.K., Keller, T., DeLuisi, J., Wuebbles, D.J., Kerr, J.B., Miller, A.J., Oltmans, S.J., Frederick, J.E., 1998. Factors affecting the detection of trends: statistical considerations and applications to environmental data. *Journal of Geophysical Research — Atmospheres* 103, 17149—17161.

Wu, Z., Huang, N.E., Long, S.R., Peng, C-K., 2007. On the trend, detrending, and variability of non-linear and non-stationary time series. *PNAS* 104, 14889-14894.

Wyoming University (WU), 2012. http://weather.uwyo.edu/surface/, accessed in December 2012.